

# PREDICTION OF IN-PHANTOM DOSE DISTRIBUTION USING IN-AIR NEUTRON BEAM CHARACTERISTICS FOR BNCS

J.M. Verbeke<sup>a,b</sup>, A. Chen<sup>a,b</sup>, J. Vujic<sup>a</sup> and K.N. Leung<sup>b</sup>

<sup>a</sup>Nuclear Engineering Department, University of California, Berkeley

<sup>b</sup>Lawrence Berkeley National Laboratory

Berkeley, CA 94720, USA

Author to whom correspondence should be sent:

J.M. Verbeke

MS 5-101

Ernest Orlando Lawrence Berkeley National Laboratory

1 Cyclotron Road

Berkeley, CA 94720

USA

email: JMVerbeke@lbl.gov

phone: (510) 495 2792

fax: (510) 486 5105

Number of pages: 22

Number of tables: 1

Number of figures: 5

## Abstract

A monoenergetic neutron beam simulation study is carried out to determine the optimal neutron energy range for treatment of rheumatoid arthritis using radiation synovectomy. The goal of the treatment is the ablation of diseased synovial membranes in joints, such as knees and fingers. This study focuses on human knee joints. Two figures-of-merit are used to measure the neutron beam quality, the ratio of the synovium absorbed dose to the skin absorbed dose, and the ratio of the synovium absorbed dose to the bone absorbed dose. It was found that (a) thermal neutron beams are optimal for treatment, (b) similar absorbed dose rates and therapeutic ratios are obtained with monodirectional and isotropic neutron beams. Computation of the dose distribution in a human knee requires the simulation of particle transport from the neutron source to the knee phantom through the moderator. A method was developed to predict the dose distribution in a knee phantom from any neutron and photon beam spectra incident on the knee. This method was revealed to be reasonably accurate and enabled one to reduce by a factor of 10 the particle transport simulation time by modeling the moderator only.

# I INTRODUCTION

Rheumatoid arthritis is a disease characterized by the inflammation of the synovial membrane or synovium, a thin tissue layer which overlays articulating joints (such as the knee and finger joints) and provides lubrication for the articulation. It results in swollen, inflamed and painful joints, which can cause loss of joint function at advanced stages. Different treatments are currently used for this disease. The most common is the administration of drugs to reduce synovial inflammation. Even though the drugs work successfully for the majority of the patients, some joints are unresponsive to this treatment and removal of the synovial membrane becomes necessary. Excision of the inflamed synovium via invasive surgery is effective in treating the disease but presents some dangers, such as infection, hemorrhage and anesthesia. Moreover, complete removal of the inflamed tissues is technically difficult due to the recesses and crevices of the joints. This synovectomy technique also incapacitates the patient during the recovery period. Radiation synovectomy using beta-emitting radionuclides presents several advantages such as success rates comparable to surgery, local anesthesia, no rehabilitation time, lower cost and a less time-consuming procedure. However, irradiation of healthy tissues by diffusion of beta-emitters away from the joint is a major concern [1, 2].

Boron neutron capture synovectomy (BNCS) [3, 4, 5, 6] is currently being investigated as an alternative treatment for rheumatoid arthritis. The treatment is similar to boron neutron capture therapy [7, 8], presently being studied for treatment of glioblastoma multiforme, a malignant brain tumor. It employs the  $^{10}\text{B}(n, \alpha)^7\text{Li}$  reaction. One of the applications of BNCS is the treatment of diseased knee joints. A boronated compound such as  $\text{K}_2\text{B}_{12}\text{H}_{12}$  is injected into the synovial membrane of the diseased knee. After injection, the knee is exposed to a low-energy neutron beam. Boron-10 atoms, with their large absorption cross section for thermal neutrons, undergo fission reactions, releasing high-energy, high-LET alpha particles and lithium nuclei. These particles deposit their energy locally (typically 2.3-2.8 MeV within 4-9  $\mu\text{m}$ ) and they damage or kill the cells along their paths. Since boron has been previously concentrated in the synovium cells, the dose given to the synovium will be significantly higher than the dose given to healthy tissues and bones. The treatment is expected to take only a few minutes of neutron irradiation time. BNCS offers the same advantages as therapies based on beta-emitting radionuclides by being non-invasive, and additionally by permitting a better control on the irradiation of healthy tissues,

since cell killing is triggered by the neutron beam and stops after irradiation.

The dose-response to a neutron beam incident on a knee depends on the neutron beam energy. In this paper, we develop a simple method to determine the dose distribution in the knee, given any neutron beam energy distribution. In the future, this method will be used to accelerate the design of beam-shaping assemblies for different candidate neutron sources for BNCS.

## II CLINICAL REQUIREMENTS

It is necessary to determine clinical criteria in order to design an efficient, practical and safe neutron beam for radiotherapy. To be efficient, the neutron beam must deliver a dose to the boron-loaded synovium sufficient to thoroughly kill the cells of the inflamed tissues. The dose required to produce a clinical effect on the synovium as estimated for beta-emitters is about 100 Gy-equivalent. Boronated compounds uptake in the synovium higher than 1000 ppm have been reported [6] in the past few years. With this localized high boron uptake, high doses to the synovial membrane can be achieved without irradiating neighboring tissues excessively.

Skin and bone are of concern. Radiation effects in the skin are non-stochastic and a mild skin reddening, which is not permanent, is observed at doses of approximately 8 Gy-equivalent [9]. Concerning the bone, potential radiation effects are stochastic indicating that the probability of cancer induction increases with the radiation dose without dose threshold [3]. Reduction of bone dose is crucial to the success of any BNCS treatment regimen.

Let  $D_{syn}$ ,  $D_{sk}$  and  $D_{bone}$  be the average absorbed synovium, skin and bone doses per neutron emitted by the source. Let  $N$  be the number of source neutrons required to reach the 100 Gy-equivalent dose in the synovium. The synovium, skin and bone doses are then given by  $N \cdot D_{syn}$ ,  $N \cdot D_{sk}$ , and  $N \cdot D_{bone}$ , respectively. In mathematical terms, the neutron beam energy  $E_{optimal}$  is optimal for BNCS treatment when

$$D_{bone}(E_{optimal}) = \min(D_{bone}(E)) \quad (1)$$

for  $0 \leq E \leq 14$  MeV, under the constraints

$$N \cdot D_{sk}(E_{optimal}) \leq 8 \text{ Gy-equivalent} \quad (2)$$

and

$$N \cdot D_{syn}(E_{optimal}) = 100 \text{ Gy-equivalent}. \quad (3)$$

The number of neutrons  $N$  is determined using Eq. 3. All the doses are scaled in such a way that Eq. 3 is verified. From Eq. 3, one can compute the time  $T$  required for treatment using

$$T = \frac{N}{S} \text{ [s]} \quad (4)$$

where  $S$  is the neutron source strength in  $s^{-1}$ .

An analysis based on two figures-of-merit has been proposed by Yanch et al. [3] to measure the beam quality. The first one is the ratio of the synovium absorbed dose to the skin absorbed dose. In order to satisfy both the 100 Gy-equivalent dose to the synovium and the 8 Gy-equivalent dose limit on the skin, this ratio should be greater than 12.5. The second is the ratio of the synovium absorbed dose to the bone absorbed dose. It is advantageous to maximize this ratio in order to limit potential cancer induction. In terms of the quantities defined above, Yanch's analysis results in the following equations for the optimization. The neutron energy  $E_{optimal}$  is optimal when

$$D_{syn}(E_{optimal})/D_{bone}(E_{optimal}) = \max(D_{syn}(E)/D_{bone}(E)) \quad (5)$$

for  $0 \leq E \leq 14$  MeV, under the constraint

$$D_{syn}(E_{optimal})/D_{sk}(E_{optimal}) \geq 100/8 = 12.5. \quad (6)$$

Besides maximizing the ratio in Eq. 5 under the constraint of Eq. 6, an ideal neutron beam must have sufficient intensity for short treatment times, though fractionated radiation schemes could be adopted.

### III DOSE COMPUTATIONS IN THE KNEE

The human knee model used in our numerical simulation is taken from Ref. [5] and is shown in Fig. 1. It is composed of concentric circles representing different layers of tissue at various depths. The outer diameter of the knee is 8.7 cm and corresponds to the approximate width of an adult human knee. Tissue layers were assigned the following thicknesses estimated using MRI data of the knee: 1.0 cm joint capsule, 0.3 cm sub-synovium, 0.15 cm synovium, 0.2 cm fluid space, 0.2 cm articular cartilage, and 5.0-cm-diam

bone. The synovium layer was therefore at the depth of 1.3 to 1.45 cm below the surface of the skin in the knee model. The estimates for elemental compositions of tissue and bone are shown in Table I. Boron-10 concentrations of 1000 ppm in the synovium and 1 ppm in all other tissues are assumed for the numerical simulations. The neutron beam direction is normal to the skin and is 8.7 cm in diameter. Neutron and photon transport in the soft tissues was simulated by the Monte-Carlo code MCNP [10]. The photon fluences computed in the volumes inside the 2.5-cm-diam cylinder intersecting the knee (see Fig. 1) are modified by the photon mass attenuation coefficients of ICRU report 46 [11] to compute the photon doses  $D_\gamma$ . Similarly, the neutron fluences are modified by the fluence-to-kerma conversion factors [11] to compute the neutron doses. All reactions happening at neutron energies less than 0.5 eV (mostly nitrogen absorption reactions) constitute the thermal neutron dose  $D_{th}$ , while all reactions above 0.5 eV (mostly proton recoil reactions) contribute to the fast neutron dose  $D_f$ . The dosimetric effect of neutrons will depend on the concentrations of  $^{10}\text{B}$  in both synovium and healthy tissues. To estimate the  $^{10}\text{B}(n, \alpha)^7\text{Li}$  contribution  $D_B$  to the dose, the neutron fluence was modified by  $^{10}\text{B}$  fluence-to-kerma conversion factors, listed in Caswell et al. [12], and then multiplied by either a factor of 1 ppm (to represent the 1  $\mu\text{g/g}$  of  $^{10}\text{B}$  in healthy tissues) or a factor of 1000 ppm (to represent the 1000  $\mu\text{g/g}$  of  $^{10}\text{B}$  in synovium). Dose-response curves depend on the type of radiation used and on the biological endpoint studied. Different radiations can be contrasted in terms of their relative biological effectiveness (RBE) compared with X rays. If a dose  $D$  of a given type of radiation produces a specific endpoint, then RBE is defined as the ratio  $\text{RBE} = D_X / D$ , where  $D_X$  is the X-ray dose needed under the same conditions to produce the same endpoint. The total absorbed tissue doses are obtained by combining the individual dose components weighted by their RBE factors, using the following equation:

$$D_{total} = RBE_B \cdot D_B + RBE_{th} \cdot D_{th} + RBE_f \cdot D_f + RBE_\gamma \cdot D_\gamma \quad [\text{Gy} - \text{equivalent per neutron}] \quad (7)$$

where the following assumptions are made:  $^{10}\text{B}$  reaction products  $RBE_B$  is 4.0, thermal neutron reaction  $RBE_{th}$  is 3.8, fast neutron reaction  $RBE_f$  is 3.8,  $RBE_\gamma$  is 1.0. The RBE values and  $^{10}\text{B}$  concentrations were taken directly from values used in Ref. [5].

## IV NEUTRON BEAM DOSE-RESPONSE

In order to predict the dose-response to any neutron energy spectrum, a large number of simulations were performed with monoenergetic neutron beams. Each simulation consisted of a 8.7-cm-diam neutron beam — which corresponds to the knee diameter — located at a distance of 1.65 cm from the surface of the knee and centered on the axis of the cylinder where the absorbed doses are computed. The neutron beam energies ranged from 0.01 eV to 14 MeV, with four energies equilogarithmically spaced per decade. This energy range covers cold, thermal, epithermal, and finally the fast neutrons produced by the D-D and D-T reactions. For each simulation, the dose-response for each reaction in Eq. 7 was determined along the centerline of the beam through the knee. A large database was constructed from which dose as a function of the energy, position, reaction, and RBE can be determined for any monodirectional neutron beam of diameter 8.7 cm incident on the knee. The only necessary input is the neutron and photon energy distributions of the beam. The dose-response to any neutron and photon spectra can be computed instantaneously using this database, since it does not require the Monte-Carlo simulation of radiation transport in the knee. A similar database can be constructed to evaluate the dose-response to any photon beam incident on the knee.

### IV.1 Analysis of the dose-response databases

A previous study by Binello et al. [6] showed that low-energy neutrons in the range from thermal energies to 1 keV provide the highest therapeutic ratios. This study was carried out for isotropic neutron beams. One could expect the neutron angular distribution to be mainly isotropic after heavy moderation by low-Z materials, which is required to slow down the high-energy neutrons produced by most neutron sources to the desired energy range. However, the presence of the collimator reduces the number of neutrons directly in line of sight with the knee to a small fraction within the solid angle formed by the exit window of the collimator, see Fig. 2. This results in a neutron beam which has a forward-peaked angular distribution. To illustrate the effect of the collimator on the directionality of the neutron beam, we consider the following example where neutrons from the D-D reaction are thermalized by a 50-cm-thick, 35-cm-diam D<sub>2</sub>O moderator (see Fig. 2), which is surrounded by a 10-cm-thick lead reflector. The reflector in turn is surrounded by a 10-cm-thick lithiated polyethylene layer. The back-reflector is a 10-

cm-thick lead layer and is followed by a 10-cm-thick lithiated polyethylene layer. The delimiter between the beam-shaping assembly (BSA) and the knee is a single 11-cm-thick lithiated polyethylene layer. The collimator is cylindrical, 8.7 cm in diameter and not lined by any material. The current-to-flux ratio, which measures beam directionality, is equal to 0.5 for a neutron beam isotropic in  $2\pi$  in the forward direction (referred to as isotropic in the remaining part of the text). It is equal to 1.0 for a monodirectional neutron beam. In our case, the ratio is equal to 0.55 before the collimator and 0.90 at the exit window of the collimator. This number reveals the strong directionality of the beam. Since a general neutron beam is partially isotropic and monodirectional, it is interesting to see whether the dose-responses for isotropic and monodirectional neutron beams are similar.

The therapeutic ratios as a function of the neutron energy are shown for both cases in Fig. 3a. The ratio of the synovium absorbed dose to the average bone absorbed dose decreases as the neutron energy increases for both beam cases. Monodirectional neutron beams are more penetrating than isotropic ones, and their synovium/bone ratios are therefore 20% lower. The ratio of the synovium absorbed dose to maximum front skin absorbed dose increases from thermal energies to 1 eV, is approximately constant between 1 eV and 0.5 keV and decreases rapidly down to 0 at about 100 keV. This ratio is slightly higher for monodirectional neutron beams than for isotropic ones. In order to satisfy the 8 Gy-equivalent dose limit on the skin dose, this ratio has to be higher than  $100/8 = 12.5$ . This condition is satisfied for all neutrons of energy lower than approximately 10 keV. In order to maximize the synovium/bone therapeutic ratio under the skin dose limit constraint, thermal neutron beams are optimal.

The dose rates per unit neutron current at the neutron source for three different positions in the knee are shown in Fig. 3b. The dose rates to the skin and bone layers indicated in the graph increase rapidly for energies above 1 keV and 10 keV, respectively. For instance, one 14.1 MeV neutron contributes as much to the skin layer dose as 500 neutrons of energy 0.1 keV in the isotropic neutron beam case. Moreover, these fast neutrons contribute less to the synovium absorbed dose than neutrons of energy 0.1 keV. For this reason and from the therapeutic ratios shown in Fig. 3a, neutrons in the energy range of 5 to 10 keV and higher are therapeutically undesirable. Fast neutron (14 MeV) currents at the entrance of the knee must be at least three orders of magnitude lower than the desired thermal neutron currents in order not to be main contributors to the skin dose and decrease the therapeutic ratios. Similar calculations can be performed for all neutron energies and one can then deduce how much each fast component of



the neutron current must be decreased to obtain reasonably good therapeutic ratios. An ideal neutron spectrum can be determined based on such an analysis.

Neutrons with energy 0.2 eV maximize the synovium dose per neutron emitted by the source. Each neutron emitted by the source delivers  $\sim 10^{-11}$  Gy-equivalent to the synovium. The number of neutrons required to reach the 100-Gy-equivalent dose in the synovium is  $10^{13}$ . Dividing by the area of the beam, this corresponds to a neutron fluence of  $1.7 \cdot 10^{11} \text{ cm}^{-2}$ , or a neutron flux of  $2.8 \cdot 10^8 \text{ cm}^{-2} \cdot \text{s}^{-1}$  for a 10-min treatment time.

Figure 4 shows the dose distribution in the knee corresponding to a monodirectional neutron beam of energy 0.031 eV. Since only neutrons are irradiating the patient's knee in this simulation study, the gamma dose is strictly induced by interactions of the neutrons with the different tissues in the knee. This induced gamma dose (mainly due to the interactions of neutrons with hydrogen) represents about 20% of the total tissue dose at the surface of the skin and 50% of the total tissue dose in the center of the knee.

## IV.2 Use of dose-response databases for the design of BSAs

These dose-response databases can be used to accelerate the design of BSAs for BNCS. MCNP is used to simulate the neutron and photon transport through the BSA. Given a neutron source strength, the neutron and photon currents and fluxes are calculated across the 8.7-cm-diam exit window at the end of the BSA, see Fig. 2. The dose-response database corresponding to the monodirectional neutron beam is then used to convert the neutron current passing through the exit window of the delimiter into a dose rate distribution in the knee. Since we are using the dose-response database corresponding to a 8.7-cm-diam monodirectional neutron beam, this conversion gives the dose rate distribution in the knee which results from a 8.7-cm-diam monodirectional neutron beam that has the same neutron current at the exit window of the delimiter as the one computed by MCNP. We will refer to it as the monodirectional neutron beam dose-response. The same procedure can be followed to compute the isotropic neutron beam dose-response using the dose-response database corresponding to the isotropic neutron beam instead of the one corresponding to the monodirectional neutron beam. To compute the dose-response of the neutron beam coming out of the delimiter (referred to as real neutron beam), which is neither monodirectional nor isotropic, we will combine the monodirectional with the isotropic neutron beam dose-responses in

such a way that the combination of them is a good estimation of the actual dose distribution in the knee.

The procedure is based on the fact that any neutron beam can be approximated by the weighted sum of a monodirectional neutron beam and an isotropic neutron beam. Different approximations are possible, the one used in this study is based on the equality of the neutron beam directionalities. The directionality  $\alpha$  of the real neutron beam — or any neutron beam — is the ratio of the neutron current density at the exit window of the delimiter to the neutron flux density at the same location, i.e.,  $J_+/\phi$ . In order to obtain the same directionality  $\alpha$  from a combination of a monodirectional neutron beam and an isotropic neutron beam, one has to combine a fraction  $2 \cdot \alpha - 1$  of the monodirectional neutron beam with a fraction  $2 \cdot (1 - \alpha)$  of the isotropic neutron beam. Indeed, by integrating the weighted sum of the angular neutron densities  $n_{monodirectional}(\theta, \varphi) = \frac{\delta(\varphi - \pi/2)}{2\pi}$  and  $n_{isotropic}(\theta, \varphi) = \frac{1}{2\pi}$  corresponding to the two beam types over all solid angles corresponding to positive currents, one obtains a neutron current

$$J_+ = \int_{\theta=0}^{\theta=2\pi} d\theta \int_{\varphi=0}^{\varphi=\pi/2} d\varphi \left[ (2 \cdot \alpha - 1) \cdot \frac{\delta(\varphi - \pi/2)}{2\pi} + 2 \cdot (1 - \alpha) \cdot \frac{1}{2\pi} \cos(\varphi) \sin(\varphi) \right] = \alpha \quad (8)$$

and a neutron flux

$$\phi = \int_{\theta=0}^{\theta=2\pi} d\theta \int_{\varphi=0}^{\varphi=\pi/2} d\varphi \left[ (2 \cdot \alpha - 1) \cdot \frac{\delta(\varphi - \pi/2)}{2\pi} + 2 \cdot (1 - \alpha) \cdot \frac{1}{2\pi} \cos(\varphi) \right] = 1 \quad (9)$$

which result in the same neutron beam directionality  $J_+/\phi = \alpha$  as the real neutron beam. It should be noted that the two angular neutron densities  $n_{monodirectional}(\theta, \varphi)$  and  $n_{isotropic}(\theta, \varphi)$  are normalized in such a way that their integral over all solid angles corresponding to positive currents is equal to 1.

The monodirectional and isotropic neutron beam dose-responses will be weighted the same way to obtain an approximation of the dose distribution in the knee for the real neutron beam. The same procedure can be used to convert the photon current at the exit window of the delimiter into a dose distribution corresponding to the photons passing through the exit window of the delimiter. Adding up the two dose distributions, we can compute the dose distribution in the knee due to the neutrons and photons going through the exit window.

This method will be referred to as "dose-response database method". It will be compared with the "full simulation method", where the neutron and photon transport simulation from the neutron source to the knee is performed entirely by the code MCNP. For both methods, different variance reduction techniques such as geometry splitting with Russian roulette, weight windows, angle biasing with DXTRAN are used to decrease the simulation time. The dose-response database method is computationally less

time-consuming than the full simulation method, it is approximately 10 times faster. The drawback of this method is that it does not account for the particles transmitted through the delimiter. Only the particles crossing the exit window are used to compute the dose-response. For this reason, the delimiter has to be designed using the full simulation method, with the goal of reducing to negligible values the radiation due to leakage through the delimiter. Once the delimiter has been shown to attenuate efficiently radiation leakage through the delimiter using the full simulation method, the dose-response database method can be used more extensively for the design of neutron beams.

Figure 5 compares the dose distributions computed using the dose-response database and full simulation methods. The D-D neutron source and BSA used for the comparison are the ones described in Sec. IV.1. This moderator composed primarily of heavy water was chosen because of its high moderating ratio and low photon production, which lead to high therapeutic ratios. For the sake of clarity, only the total tissue absorbed dose is shown for the computations with the dose-response database method. The delimiter used for this simulation is very efficient for the attenuation of neutron fluxes. Leakage of photons through the delimiter is not of primary concern, due to the low level of photon fluxes at the end of the moderation. Even without the delimiter, photons coming from this moderator contribute less than 5% of the total dose in the knee. We observe in Fig. 5 that the two methods provide significantly identical total absorbed doses for most depths in the knee. Further comparisons to validate the method are planned, and results will be reported at the appropriate time. In the case of the dose distribution corresponding to the pure thermal neutron beam shown in Fig. 4 — which is close to an ideal neutron beam —, the main contributor to the total dose is the dose corresponding to the thermal neutrons. In Fig. 5, the total absorbed dose is mostly due to the fast component of the neutron beam through proton recoil reactions.

## V CONCLUSION

Using Monte Carlo simulations to model neutron beam interaction with a phantom knee, guidelines were developed for determining the optimal neutron beam energy for delivering dose to the target area, the synovium. Two figures-of-merit are used to measure the beam quality, the ratio of the synovium absorbed dose to the skin absorbed dose, and the ratio of the synovium absorbed dose to the bone absorbed dose.

It was found that a thermal neutron beam is optimal for BNCS treatment. Similar absorbed dose rates and therapeutic ratios were obtained with monodirectional and isotropic neutron beams. The thermal neutron flux required to deliver 100 Gy-equivalent to the synovium in 10 min is approximately  $2.8 \cdot 10^8 \text{ cm}^{-2} \cdot \text{s}^{-1}$ . The calculated dose rates and ratios depend on the  $^{10}\text{B}$  concentrations in the synovium and healthy tissues. A  $^{10}\text{B}$  concentration of 1000 ppm was assumed in the synovium, while 1 ppm was assumed in the healthy tissues and bone.

Computation of the dose distribution in the knee requires the simulation of the neutron and photon transport from the neutron source to the knee phantom through the complex beam-shaping assembly. A method — namely the dose-response database method — was developed to predict the absorbed dose distribution in the knee based on any neutron and photon spectra incident on the knee. This method enables one to reduce by a factor 10 the neutron and photon transport simulation time by modeling the transport in the moderator only. Good agreement was observed between dose distributions computed using this method and dose distributions computed using simulation of the entire model, i.e., moderator and knee phantom.

## VI ACKNOWLEDGEMENTS

This work is partly supported by the US Department of Energy under contract number DE-AC03-76SF00098.

## List of Tables

I	Density and elemental composition of bone and soft tissue in weight percentages. . . . .	15
---	--	----

## List of Figures

1	Cross-section view of the cylindrical knee model used in the MCNP simulations. Absorbed doses are computed as a function of the depth within the 2.5-cm-diam cylinder intersecting the different tissue layers. . . . .	16
2	Sample beam-shaping assembly (BSA). . . . .	17
3	(a) Therapeutic ratios and (b) absorbed dose rates per unit neutron current at the neutron source as a function of the neutron beam energy for isotropic and monodirectional neutron beams. . . . .	18
4	Absorbed dose rates versus depth for a 8.7-cm-diam monodirectional neutron beam of energy 0.031 eV. A neutron source strength of $7 \cdot 10^{11} \text{ s}^{-1}$ was used. . . . .	19
5	Comparison of the dose-response database method with the full simulation method for the computation of the absorbed dose rates. A D-D neutron source of strength of $7 \cdot 10^{11} \text{ s}^{-1}$ was used. . . . .	20

Element	articular cartilage	bone	joint fluid	tissue
Hydrogen	9.60	3.40	11.10	10.00
Carbon	9.90	15.50	-	14.90
Nitrogen	2.20	4.20	-	3.50
Oxygen	74.40	43.50	88.90	71.60
Magnesium	0.50	-	-	-
Phosphorous	-	0.20	-	-
Sulfur	2.20	10.30	-	-
Calcium	0.09	22.50	-	-
Chlorine	0.03	-	-	-
Density [g/cm <sup>3</sup> ]	1.10	1.92	1.00	1.00

Table I: Density and elemental composition of bone and soft tissue in weight percentages.

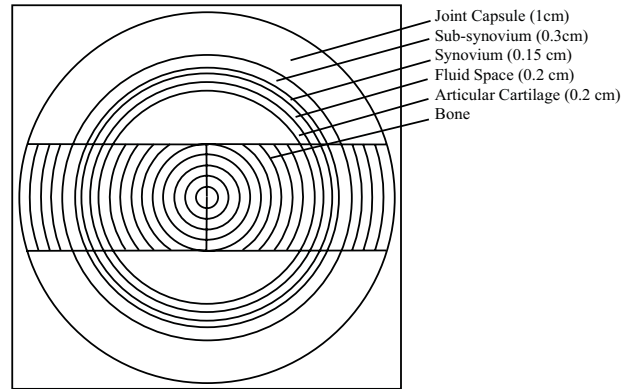


Figure 1: Cross-section view of the cylindrical knee model used in the MCNP simulations. Absorbed doses are computed as a function of the depth within the 2.5-cm-diam cylinder intersecting the different tissue layers.



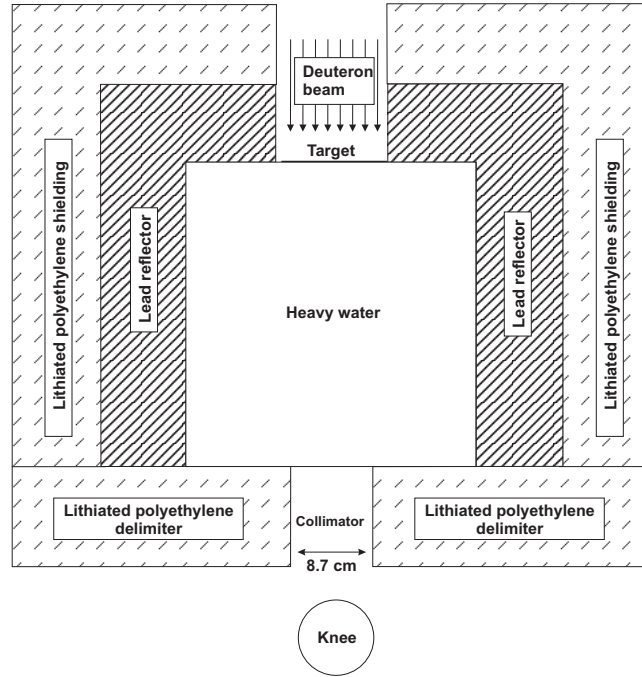
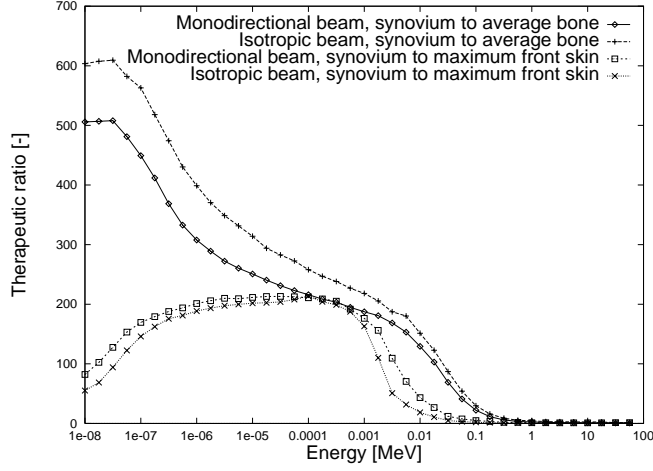
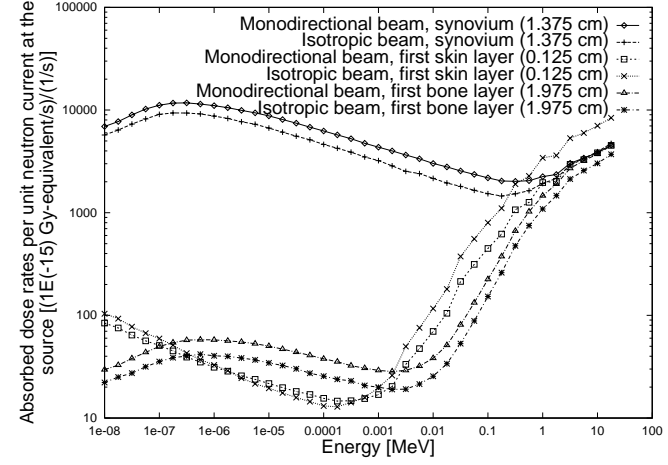


Figure 2: Sample beam-shaping assembly (BSA).

J.M. Verbeke - Prediction of in-phantom neutron beam characteristics using in-air figure-of-merit for BNCS



(a)



(b)

Figure 3: (a) Therapeutic ratios and (b) absorbed dose rates per unit neutron current at the neutron source as a function of the neutron beam energy for isotropic and monodirectional neutron beams.

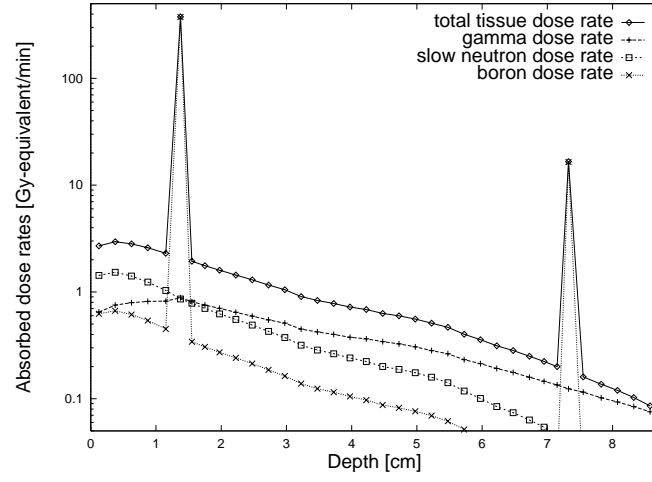


Figure 4: Absorbed dose rates versus depth for a 8.7-cm-diam monodirectional neutron beam of energy 0.031 eV. A neutron source strength of  $7 \cdot 10^{11} \text{ s}^{-1}$  was used.

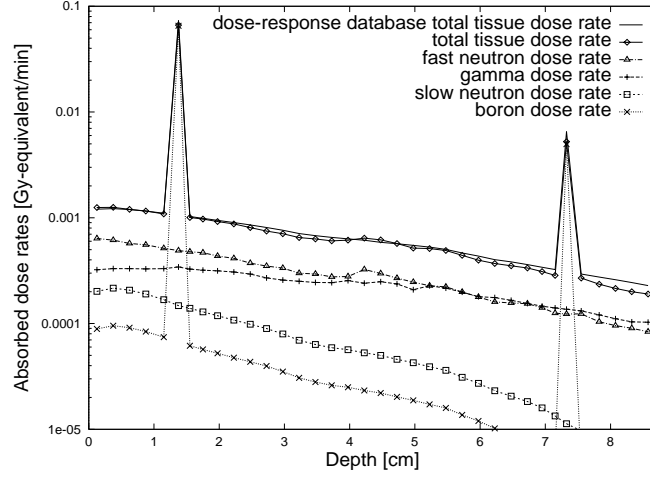


Figure 5: Comparison of the dose-response database method with the full simulation method for the computation of the absorbed dose rates. A D-D neutron source of strength of  $7 \cdot 10^{11} \text{ s}^{-1}$  was used.

## References

- [1] M. Davis, M. Chinol, "Radiopharmaceuticals for Radiation Synovectomy: Evaluation of Two Yttrium-90 Particulate Agents," J. Nucl. Med., **30**, 1047-1055 (1989).
- [2] J. Noble, A.G. Jones, M.A. Davis, C.B. Sledge, R.I. Kramer, E. Livni, "Leakage of Radioactive Particle Systems from a Synovial Joint Studied with a Gamma Camera," J. Bone Joint Surg. (Am), **65-A**, 381-389 (1983).
- [3] J.C. Yanch, S. Shortkroff, R.E. Shefer, S. Johnson, E. Binello, D. Gierga, A.G. Jones, G. Young, C. Vivieros, A. Davidson, and C. Sledge, "Boron Neutron Capture Synovectomy: Treatment of Rheumatoid Arthritis Based on the  $^{10}\text{B}(n, \alpha)^7\text{Li}$  Nuclear Reaction," Med. Phys., **26**, 364-375 (1999).
- [4] Harris, D. Edward, Rheumatoid Arthritis, Saunders, Philadelphia (1997).
- [5] J.C. Yanch, R.E. Shefer, and E. Binello, "Design of Low-Energy Neutron Beams for Boron Neutron Capture Synovectomy," Proc. Int. Conf. Neutrons in Research and Industry, Crete, Greece, June 9-15, 1996, SPIE 2867, p. 31-40 (1996).
- [6] E. Binello, S. Shortkroff, A. Jones, C. Viveiros, A. Ly, C.B. Sledge, A. Davidson, R.E. Shefer, and J.C. Yanch, "Research in Boron Neutron Capture Synovectomy," Proc. Int. Conf. Neutrons in Research and Industry, Crete, Greece, June 9-15, 1996, SPIE 2867, p. 68-71 (1996).
- [7] D.T. Ingersoll, C.O. Slater, E.L. Redmond, II, and R.G. Zamenhof, "Comparison of TORT and MCNP Dose Calculations for BNCT Treatment Planning," Proc. 7<sup>th</sup> Int. Symp. Neutron Capture Therapy for Cancer, Zurich, Switzerland, Sept. 4-7, 1996, Trans. American Nuclear Society, vol. 75, 36-37 (1996).
- [8] R.F. Barth, A.H. Soloway, R.G. Fairchild, and R.M. Brugger, "Boron neutron capture therapy: realities and prospects", Cancer, **70**, 2995-3001 (1992).
- [9] A.H.W. Nias, An Introduction to Radiobiology, John Wiley & Sons, New York (1990).
- [10] J.F. Briesmeister, "MCNP — A General Monte Carlo N-Particle Transport Code, Version 4B," LA-12625-M, Los Alamos National Laboratory (1997).

- [11] "Photon, Electron, Proton and Neutron Interaction Data for Body Tissues," ICRU 46, International Commission on Radiation Units and Measurements (1992).
- [12] R.S. Caswell, J.J. Coyne, and M.L. Randolph, "Kerma Factors of Elements and Compounds for Neutron Energies Below 30 MeV," Int. J. Appl. Radiat. Isot., **33**, 1227-1262 (1982).